Measurement of the optical absorption coefficient of a liquid by use of a time-resolved photoacoustic technique

Yaochun Shen, Zuhong Lu, Stephen Spiers, Hugh A. MacKenzie, Helen S. Ashton, John Hannigan, Scott S. Freeborn, and John Lindberg

A time-resolved photoacoustic technique has been applied to the study of dissolved and dispersed absorbers in aqueous systems. The temporal pressure profiles generated from colloidal graphite and glucose solutions were measured, and it was found that the amplitude of the photoacoustic signal of both the glucose and the colloidal graphite solutions increase linearly with concentration and that acoustic signal time delay yields the acoustic velocity. The logarithm of the photoacoustic signal amplitude changes linearly with the time delay, with a slope that is proportional to the product of the acoustic velocity and the optical absorption that can thus be determined. © 2000 Optical Society of America

OCIS codes: 300.0300, 300.6430.

1. Introduction

The photoacoustic technique is unusual amongst spectroscopic measurements in that it inherently involves important physical and thermal parameters as well as the basic optical properties of the material. The amount of absorbed optical energy is determined by the optical absorption coefficient, but the specific heat, thermal expansion coefficient, density, and the bulk modulus of the medium determine the subsequent generation of the photoacoustic wave. For example, the photoacoustic response from water is relatively poor, and this aspect can be used to advantage in the detection of analytes, e.g., hydrocarbons in water,[1] where the combination of physical parameters for hydrocarbons may combine to enhance the photoacoustic response. A disadvantage of the photoacoustic technique however, is the possible difficulty of determining the optical absorption coefficient for direct comparison with results from other spectroscopic techniques. Although the same spectroscopic features may appear in photoacoustic spectra as in absorption spectroscopy, the relative amplitudes of the spectral peaks may be significantly different owing to the involvement of physical parameters. The measurement of the first cycle, peak-to-peak amplitude of the measured photoacoustic signal contains useful information for concentration measurement of analytes such as hydrocarbons[1] and glucose[2] but does not directly yield information regarding the determination of the optical absorption coefficient. In this paper we show how a simple temporal analysis of the rising front of the photoacoustic signal may be correlated with the optical absorption coefficient for both dispersed and dissolved analytes. Variants of this technique have been previously used to investigate the temporal profile of the acoustic pulse[3] and to establish the validity of the basic principle.

2. Theory Outline

If we assume that the laser beam is incident from the $-x$ direction onto the sample surface at $x = 0$ at time $t = 0$, the one-dimensional wave equation for particle displacement $\xi(x, t)$ in a liquid is[4]

$$\frac{\partial^2 \xi}{\partial x^2} - \frac{1}{\nu^2}\frac{\partial^2 \xi}{\partial t^2} = \frac{\beta}{C_p}\frac{\partial \phi}{\partial x}, \tag{1}$$

where ν is the acoustic velocity; β, the thermal expansion coefficient; C_p, the specific heat at constant pressure; and ϕ, the optical energy absorbed per unit mass.

We also assume that the laser pulse has a rectangular temporal profile of time duration τ and a total incident energy per unit area E_0 and that it is inci-

Y. Shen and Z. Lu are with the National Laboratory of Molecular and Biomolecular Electronics, Southeast University, Nanjing 210096, China. S. Spiers, H. A. MacKenzie (h.a.mackenzie@hw.ac.uk), H. S. Ashton, J. Hannigan, S. S. Freeborn, and J. Lindberg are with the Department of Physics, Heriot Watt University, Riccarton, Edinburgh EH14 4AS, United Kingdom.

Received 27 March 2000.
0003-6935/00/220001-06$15.00/0

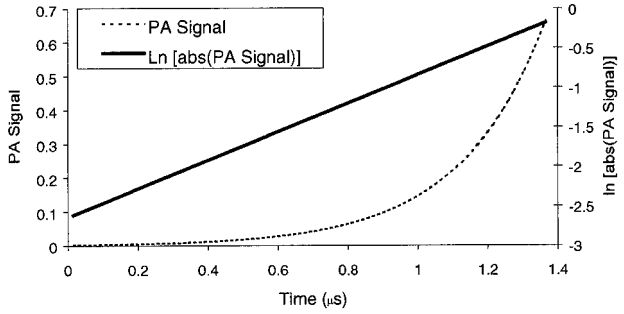

Fig. 1. Calculated photoacoustic signals with a one-dimensional theoretical model. Typical photoacoustic signal of a liquid generated by laser pulses, dashed curve; and logarithm of the photoacoustic signal, which is proportional to the time, solid line.

dent at a surface for which the boundary condition is $p(x, t) = 0$. It is assumed that $\alpha x \gg 1$ and that the absorption length α^{-1} is negligible compared with the acoustic source diameter. Investigators[4–7] have found solutions of the one-dimensional wave equation (1) in forms similar to that shown below. Solutions for the resultant pressure pulse $p(x, t)$ are of the form[4]:

$$p(x, t) = \sigma \begin{cases} \exp(\alpha \nu t')[1 - \exp(-\alpha \nu \tau)] & t' < 0 \\ \exp(-\alpha \nu t') - \exp(\alpha \nu [t' - \tau]) & 0 < t' \le \tau \\ \exp(-\alpha \nu t')[1 - \exp(\alpha \nu \tau)] & t' > \tau \end{cases}. \quad (2)$$

For the solutions of Eq. (2) to be simplified, a reduced time is defined $t' = t - x/\nu$, and

$$\sigma = \frac{\nu \beta E_0}{2 C_p \tau}. \quad (3)$$

It can be seen from the solutions of Eq. (2) that the initial rising front of the pressure pulse $p(x, t)$ has an exponential dependence, as shown in Fig. 1.

The logarithm of the resultant pressure pulse $p(x, t)$ is shown in Eq. (4):

$$\ln[p(x, t)] = \begin{cases} \ln(\sigma) + \alpha \nu t' + \ln[1 - \exp(-\alpha \nu \tau)] & t' < 0 \\ \ln(\sigma) + \ln[\exp(-\alpha \nu t') - \exp(\alpha \nu [t' - \tau])] & 0 < t' \le \tau \\ \ln(\sigma) - \alpha \nu t' + \ln[1 - \exp(\alpha \nu \tau)] & t' > \tau \end{cases}. \quad (4)$$

In Eq. (4), in all cases, the logarithm of the pressure pulse logarithmically depends on the combination of physical parameters represented by σ, and, in the cases for which $t' < 0$ and $t' > \tau$, the logarithm of the pressure pulse linearly depends on the product of the optical absorption coefficient, α, and the acoustic velocity, ν. The third term of these solutions is independent of x and t' and may be considered non-time-dependent for a fixed laser pulse duration, although it generates a baseline change with changing optical absorption.

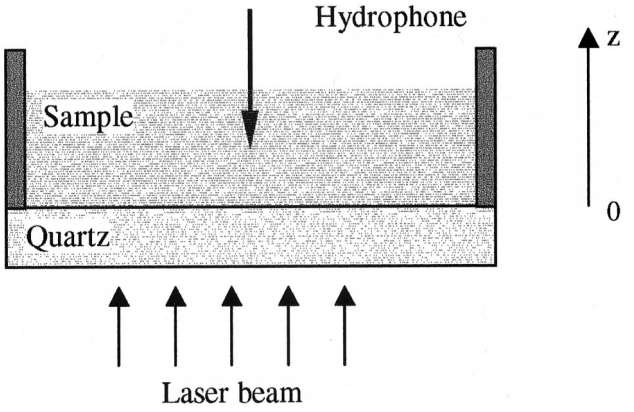

Fig. 2. Schematic representation of time-resolved photoacoustic technique.

3. Experiment

The experimental results described in Section 4 are for the cases in which the optical absorption may be due to dispersed or dissolved components. Figure 2 shows the schematic representation of the experimental setup for time-resolved photoacoustic spectroscopy. A laser pulse was directed through the quartz window, and the acoustic signal was detected with a sensitive, broad-bandwidth hydrophone. The near-infrared optical source used in this study was a MOPO laser system (MOPO-710 Spectra-Physics), which provided laser pulses with a pulse duration of approximately 10 ns at a repetition rate of 10 Hz in the near-infrared wavelength range from 800 to 2100 nm. The laser pulse was delivered to the sample by a fiber-optic delivery system, which also served to improve the beam profile and the directional stability of the laser beam. A digitizing oscilloscope (Tektronix TDS 460) was used to capture single-shot signals, which were averaged over 100 pulses to reduce the random noise effects. A wide-bandwidth (5 MHz) hydrophone was used to measure the photoacoustic pressure waves. An optical energy monitor based on a neutral density filter with a piezoelectric transducer bonded onto it was used to measure the energy of each laser pulse, and the energy monitor signal was then used to normalize the photoacoustic signal.

Three different parameters can be determined from an analysis of the temporal profile of the experimental photoacoustic signal:

(i) The time delay between the optical pulse and the detection of the photoacoustic signal is a transit time that is determined by the distance between the optical interaction region and the hydrophone. Thus the sample's sound velocity, ν, may be determined by the temporal peak position of the photoacoustic signal relative to the optical signal. This time delay changes if the changing analyte concentration also changes the elastic properties of the medium.

(ii) The amplitude of the photoacoustic signal is proportional to σ [see Eq. (3)], which may be influ-

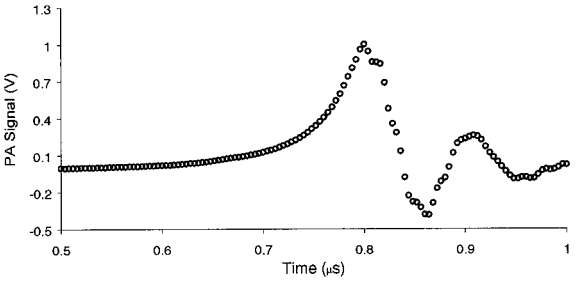

Fig. 3. Normalized photoacoustic signal.

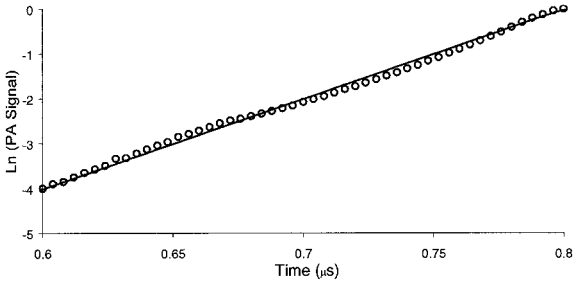

Fig. 4. Logarithm of the photoacoustic signal in Fig. 3.

enced by physical changes associated with concentrations of components in the system. Thus by means of calibration, the peak-to-peak amplitude of the photoacoustic signal may be used to determine the analyte concentration. There are also geometric effects that occur owing to the changes in absorption length as the analyte concentration changes; however, they are not a significant factor in the experiments described here.

(iii) The logarithm of the amplitude of the photoacoustic signal is proportional to the reduced time t' with a slope of αv. Thus with knowledge of v as described in Eq. (1) and for a specific measuring position (constant x), the optical absorption coefficient α may be determined. The form of this relation is shown in Fig. 1. This analysis has been used in a similar approach in time-resolved, $R(r, t)$, reflectance measurements[8] in which r is the source-to-detector separation and t is the time delay after the optical pulse. In addition, by use of the asymptotic slope of the logarithm of the temporal profile, it was possible to determine the optical absorption coefficient.

4. Results

A. Dispersed Absorber (Colloidal Graphite)

To demonstrate the capability of the time-resolved photoacoustic technique for optical absorption coefficient measurement with dispersed absorbers, we studied various concentrations of colloidal graphite. These samples were prepared, and a range of optical absorption coefficients from 28.0 to 122.6 cm^{-1} were obtained. Figure 3 shows a typical photoacoustic signal obtained by irradiation of a colloidal graphite suspension in water with a laser pulse (wavelength 900 nm, energy fluence 4.0 mJ/cm^2) through the quartz window.

The photoacoustic signal consists of two distinct parts. The initial exponential rising part relates to the depth distribution, the laser beam profile, and the absorbed laser energy in the sample. The photoacoustic signal contributions from the extreme of the depth distribution nearest to the hydrophone are the first to arrive at the detector, and those contributions from the region near to the window are the last to arrive at the detector. The second part comes from the subsequent rarefaction associated with propagation of the acoustic pulse.

By changing the position of the hydrophone detector and monitoring the corresponding change in the peak position of the measured photoacoustic signal, we determined the sound velocity of the sample to be 1481.5 m/s. This can be compared with the literature value for the sound velocity in distilled water (1482.34 m/s) at a temperature of 20 °C.[9]

The optical absorption coefficient of the sample may be determined from the photoacoustic signal by our fitting the logarithm of the photoacoustic signal amplitude as a linear function of time, as shown in Fig. 4. The slope of the best-fit line gives the product of the sound velocity v and the optical absorption coefficient α of the sample. Thus the optical absorption coefficient of the colloidal graphite suspension was determined to be 80.9 cm^{-1}, compared with a value of 84.5 cm^{-1} as measured by a Shimadzu 3000 NIR Spectrometer. This 5% discrepancy is consistent with the accumulated errors involved in both measurements and mainly from limitations of temperature control.

The photoacoustic signals from various colloidal graphite suspensions in water were measured, and it was found that all the photoacoustic signals for various graphite suspensions had the same temporal peak position within the experimental accuracy of 4 ns. Thus, since the sound velocity determines the peak position of the photoacoustic signal, all the colloidal graphite suspensions have the same sound velocity, although they have different concentrations of graphite.

Figure 5 shows the logarithm of the photoacoustic signal versus time and, as expected, the logarithm of the photoacoustic signal changes linearly with time. In addition, the optical absorption coefficients of various colloidal graphite samples were measured with a Shimadzu 3000 NIR Spectrometer. Figure 6 shows the optical absorption coefficient of the graphite solution determined with the time-resolved technique plotted against the optical absorption coefficient determined with the Shimadzu spectrometer. The best-fit line is shown with a correlation coefficient of 0.97. We are confident that this correlation could be improved with closer control of the experimental parameters, including better temperature regulation.

B. Dissolved Absorber (Glucose in Solution)

We prepared glucose solutions in the concentration range from 1 to 15 g/dl by diluting a preprepared 30 g/dl D-glucose solution with distilled water. In all

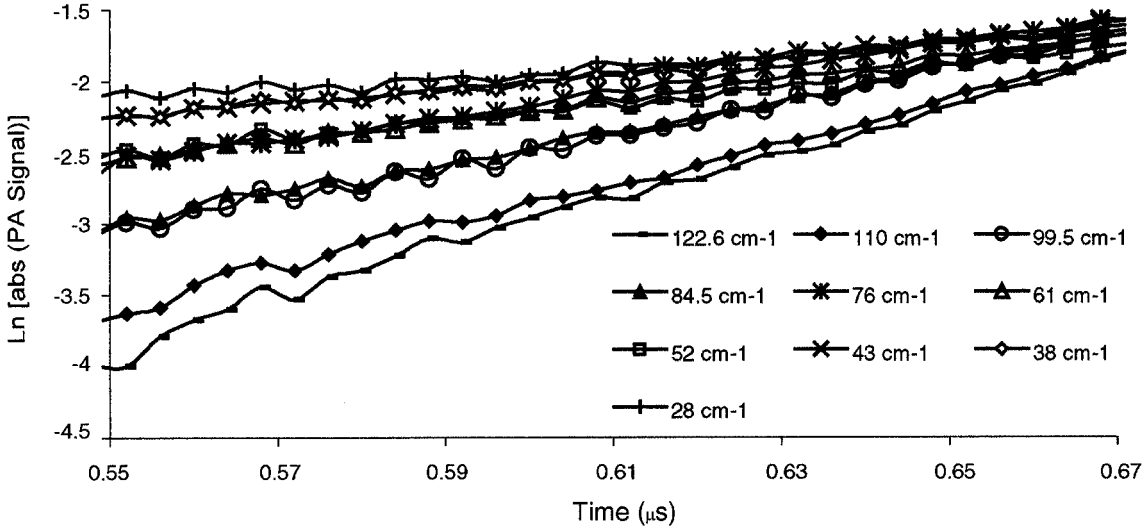

Fig. 5. Logarithm of the photoacoustic signals measured at a wavelength of 900 nm from colloidal graphite with optical absorption coefficients from 28.0–123.0 cm^{-1}.

experiments, we controlled the sample temperature at 23 °C with an accuracy of 0.1 °C to minimize the effect of any temperature change.

Figure 7 shows the logarithm of the measured photoacoustic signals (wavelength of 1450 nm, energy fluence 2.0 mJ/cm^2). As expected, the amplitude of the photoacoustic signal increases with the glucose concentration, which is consistent with the previous results measured with a piezoelectric transducer.[2,10]

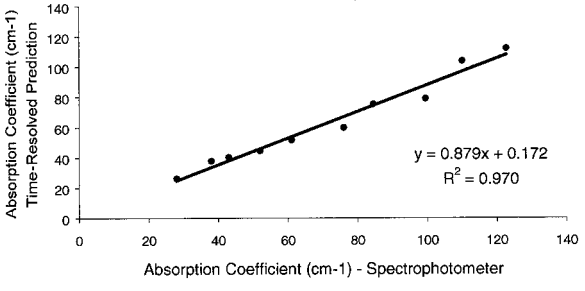

Fig. 6. Slope of the logarithm of the photoacoustic signal versus optical absorption coefficient of colloidal graphite samples. The optical absorption coefficient was measured with a Shimadzu 3000 NIR Spectrometer. The solid line represents the best-fit line to that data.

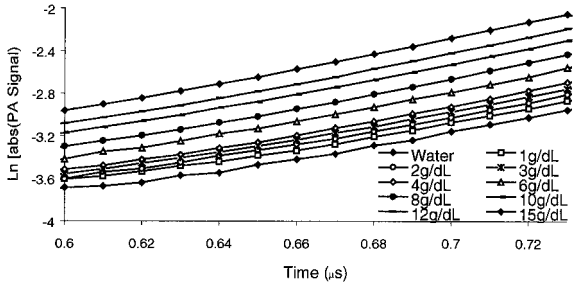

Fig. 7. Log profile of the photoacoustic signals measured at 1450 nm from glucose solution with a concentrations from 0.0–15.0 g/dl.

The change of photoacoustic signals for different glucose concentration at a wavelength of 1450 nm is plotted in Fig. 8 to show their concentration dependence. A linear response is evident in the whole concentration range investigated. In addition, it can also be seen from Fig. 8 that the temporal position of the photoacoustic peak signal changes linearly with glucose concentration, indicating that the sound velocity of the solution increases with glucose concentration at a fixed slope of 0.15% $(g/dl)^{-1}$. This is in contrast to the colloidal graphite results in which the sound velocity does not change with the graphite concentration in the concentration range investigated. For glucose solutions, the displacement of water molecules by much larger glucose molecules causes changes of the elastic properties of the solution, whereas for dispersed colloidal graphite samples, the graphite particles do not influence the acoustic propagation properties of the water.

As stated previously, the logarithm of the photoacoustic signal changes linearly with time, and the slope of the best-fit line is the product of the sound velocity v and the optical absorption coefficient α. The slopes of these linear fits, measured for various

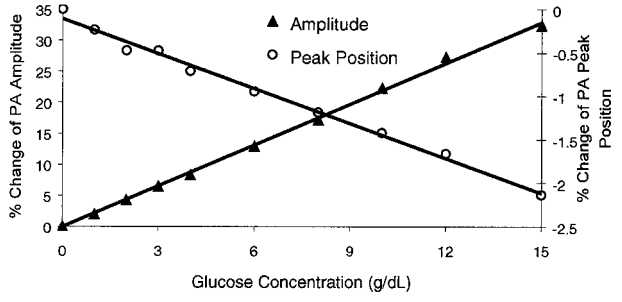

Fig. 8. Glucose concentration dependence of the amplitude and the peak position changes of the photoacoustic signals at 1450 nm. The solid line represents the best-fit line to that data.

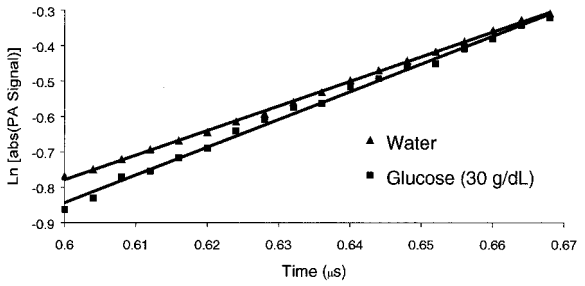

Fig. 9. Log profile of the photoacoustic signals obtained at a wavelength of 2150 nm from water and glucose solution with a concentration of 30 g/dL.

glucose concentrations, were calculated. The slopes of different glucose samples remain constant with an experimental error of approximately 3%. This implies that the optical absorption coefficient decreases with the glucose concentration at this wavelength (1450 nm) as the sound velocity increases with the glucose concentration, so that the product $\alpha\nu$ remains constant. At this wavelength (1450 nm), the optical absorption coefficient of glucose solutions consists of two opposing components. The first component is an increase due to optical absorption by the glucose molecule that increases with glucose concentration, and the second is a decrease due to the displacement of water molecules (molecular weight 18) with larger glucose molecules (molecular weight 180), causing a decrease of the optical absorption coefficient of the glucose solution. This effect can be observed at wavelengths near 1400 nm, where a strong first overtone absorption feature of the O—H bond can be found.[11] Therefore, we conclude that at 1450 nm, the net optical absorption coefficient decreases with the glucose concentration with a rate of approximately $-0.15\%\ (\mathrm{g/dl})^{-1}$.

There is also a combination band absorption region in the glucose spectrum near 2260 nm, which we accessed with a wavelength of 2150 nm. Figure 9 shows the log profile of the photoacoustic signals obtained from the water and glucose solution with a concentration of 30 g/dL. Because of the limited energy of the MOPO laser system at this wavelength, the laser beam was slightly focused to improve the signal-to-noise ratio. Therefore in this particular case the experimental results are rather qualitative. Nevertheless, the linear plots in Fig. 9 clearly illustrate that the slope of the logarithm of the photoacoustic signal depends on the glucose concentration, without the strongly opposing displacement effect that was previously observed.

5. Discussion

Compared with conventional optical spectroscopic techniques, the time-resolved photoacoustic technique has several advantages. For example, the technique is less susceptible to scattering as the photoacoustic effect is nondirectional, and the energy conversion process continues even if part of the light is scattered. In contrast, conventional optical spectroscopic techniques rely on the direct detection of transmitted light. The photoacoustic technique is also advantageous for samples with high optical absorption where the transmission of light through the sample is impossible and single surface measurements are advantageous.

Time-resolved photoacoustic techniques have been used previously to investigate a multilayer system of gels of different optical absorptions,[12] and each layer was distinguished by characteristic differences in the photoacoustic signal. With simultaneous measurement of the acoustic velocities, this technique could be extended to allow calculation of the optical absorption coefficient in each layer. Similarly, the layered structure of tissue has been investigated with a time-gated optical photoacoustic detection scheme,[13] and this type of measurement could lend itself to further analysis if the current technique is applied.

The simplicity of the current technique may be of particular importance in optical tissue imaging in which the differing optical properties of the tissue as the laser light penetrates from the skin into the capillary structure and veins may be detected as characteristic gradient changes in the processed photoacoustic traces. In addition, the technique may be useful in the quality control of multilayered products in which the optical absorption coefficient relates directly to the composition of each layer.

6. Conclusions

The time-resolved photoacoustic technique has been successfully applied to the study of dispersed and dissolved absorbers in aqueous systems. The first cycle amplitude of the photoacoustic signal, for both a dispersed absorber (colloidal graphite) and a dissolved absorber (glucose in solution), was found to increase linearly with concentration. In addition, a time-resolved study showed that the logarithm of the photoacoustic pressure amplitude, which develops in the rising front of the photoacoustic signal, changes linearly with elapsed time. This linear relation has a gradient that corresponds to the product of the optical absorption coefficient and the sound velocity.

The sound velocity of the sample was accurately determined by the peak position of the photoacoustic signal relative to the optical pulse, and from this data, the optical absorption coefficient could be calculated. In future research, this technique will be applied to the study of layered structures and tissue systems.

The authors thank the British Diabetic Association for its earlier support for this study. We also acknowledge the experimental assistance of Alistair Low.

References

1. S. S. Freeborn, J. Hannigan, F. Greig, R. A. Suttie, and H. A. MacKenzie, "A pulsed photoacoustic instrument for detection of crude oil concentrations in produced water," Rev. Sci. Instrum. **69,** 3948–3952 (1998).

2. G. B. Christison and H. A. MacKenzie, "Laser photoacoustic determination of physiological glucose concentrations in human whole blood," Med. Biol. Eng. Comput. **31,** 284–290 (1993).
3. G. J. Diebold and T. Sun, "Properties of photoacoustic waves in one, two, and three dimensions," Acoustica **80,** 339–351 (1994).
4. E. F. Carome, N. A. Clark, and C. E. Moeller, "Generation of acoustic signals in liquids by ruby laser-induced thermal stress transients," Appl. Phys. Lett. **4,** 95–97 (1964).
5. L. S. Gournay, "Conversion of electromagnetic to acoustic energy by surface heating," J. Opt. Soc. Am. **40,** 1322–1330 (1966).
6. L. V. Burmiistrova, A. A. Karabutov, A. I. Portnyagin, O. V. Rudenko, and E. B. Cherepetskaya, "Method of transfer functions in problems of thermooptical sound generation," Sov. Phys. Acoust. **24,** 369–374 (1978).
7. D. A. Hutchins, "Mechanisms of pulsed photoacoustic generation," Can. J. Phys. **64,** 1247–1264 (1986).
8. G. W. C. Kay and T. H. Laby, *Tables of Physical and Chemical Constants and Some Mathematical Functions,* 16th ed. (Longman Scientific and Technical, Essex, UK, 1995).
9. B. Chance, S. Nioka, J. Kent, K. McCully, M. Fountain, R. Greenfeld, and G. Holtom, "Time resolved spectroscopy of hemoglobin and myoglobin in resting and ishemic muscle," Anal. Biochem. **174,** 698–707 (1988).
10. H. A. MacKenzie, H. S. Ashton, S. Spiers, S. S. Freeborn, Y. C. Shen, J. Hannigan, J. Lindberg, and P. Rae, "Advances in photoacoustic non-invasive glucose testing," Clin. Chem. **45,** 1587–1595 (1999).
11. O. S. Khalil, "Spectroscopic and clinical aspects of noninvasive glucose measurements," Clin. Chem. **45,** 165–177 (1999).
12. A. A. Karabutov, N. B. Podymova, and V. S. Letokhov, "Time-resolved laser optoacoustic tomography of inhomogeneous media," Appl. Phys. B **63,** 545–563 (1996).
13. G. Paltauf and H. Schmidt-Kloiber, "Measurement of laser-induced acoustic waves with a calibrated optical transducer," J. Appl. Phys. **82,** 1525–1531 (1997).